Electronic properties of zero-layer graphene on 6H-SiC(0001) substrate decoupled by silicon intercalation

G. Silly, G. Li, Yannick J. Dappe

Electronic properties of zero-layer graphene on 6H-SiC(0001) substrate decoupled by silicon intercalation

M. G. Silly,[a] G. Li[a] and Y. J. Dappe[b]*

Graphene exhibits electronic properties that are very sensitive not only to defects but also to the interaction with extra molecules or atoms and underlying substrate. To overcome this limitation for application and mass device production, various methods have been investigated to decouple graphene from substrate and to form quasi-free standing layer. Silicon has shown to be able to softly decouple the zero-layer graphene from the substrate. However, the electronic properties of decoupled zero-layer graphene (ZLG) by silicon intercalation on 6H-SiC(0001) stay unknown. The decoupling process of the ZLG terminated surface happens at lower temperature compared with ZLG covered by 1 monolayer graphene. The presence of extra graphene layer appears to be of an impediment to silicon intercalation. The decoupled ZLG exhibits electronic properties of a quasi-free-standing monolayer graphene. *Ab initio* calculation corroborates the experimental data and confirms the evolution of the ZLG band structure with silicon intercalation. Copyright © 2014 John Wiley & Sons, Ltd.

Keywords: graphene; electronic properties; SiC

Introduction

A graphene sheet constitutes a two-dimensional layer, formed by sp^2-hybridized carbon atoms arranged in a honeycomb lattice. The band structure of graphene is governed by massless Dirac particles and exhibits characteristic linear band dispersion near the K-point linked to the half-filled π bonds.[1] This singular electronic structure sparks off novel electronic properties such as room temperature quantum Hall effect,[2] Klein tunneling[3] and high carrier mobility greater than in any known semiconductor.[4] Compatible with existing electronic device technology, graphene synthesis on SiC substrate is one of the most promising approaches for uniform coverage and structural coherence at wafer scale, a key factor to maximize the mobility and uniformity essential for applications.[5,6] Moreover, the use of wide-bandgap semiconductor SiC as semi-insulating substrate avoids hazardous transfer of the graphene layer to another insulating substrate at the origin of potential decrease in graphene electronic performances.[7] In addition, electronic properties of monolayer (ML) graphene, such as doping and electronic transport, are extremely dependent on the chemical nature of the interface. In fact, graphene grown on SiC(0001) Si-face exhibits mobilities an order of magnitude lower than on SiC(000-1) C-face, although structural graphene film quality appears comparable.[8] Hence, the control of the electronic properties of graphene layer appears to be of fundamental importance for the development of graphene electronics.[6] Therefore, in order to modify the graphene electronic properties, successful species intercalation as H,[9] O,[10] F,[11] Au,[12] Li,[13] Ge [14] and Si[15,16] has shown the high versatility of graphene doping from n-doped or p-doped materials to neutral quasi-free-standing graphene layer. As one ML graphene decoupling has been intensively investigated, zero-layer graphene or buffer layer decoupling process is still controversial, because of the complex covalent bonding between the zero-layer graphene and the substrate.[17,18] Recently, a significant

study has been carried out on one ML graphene decoupling by silicon intercalation. The authors have also evidenced the decoupling of ZLG into graphene by Low Energy Electron Diffraction (LEED).[15] Nevertheless, the electronic properties of the resulting decoupled graphene layer remains unknown. The determination of the electronic properties is of crucial interest for potential applications as silicon intercalation is compatible with current electronic technology.

Here, we present a UHV study of the buffer layer decoupling from the SiC substrate by Si intercalation. We have investigated the evolution of the electronic properties of the ZLG by means of high-resolution photoemission spectroscopy (HRPES) and angle-resolved photoemission spectroscopy (ARPES) induced by silicon intercalation. The ZLG exhibits the typical linear dispersion along the Γ–K direction characteristic of a decoupled graphene layer. The decoupled layer presents a slight n-doping. *Ab initio* calculations confirm the transition from semiconducting to metallic behavior of the terminated carbon layer.

Methods

The experiments were performed using an on-axis-oriented n-type 6H-SiC(0001) research grade substrate with polished silicon face. The SiC substrate, initially outgassed at 600 °C for 12 h in a base pressure of 5×10^{-10} mbars, is flashed in a pressure better than 3×10^{-10} mbars at a temperature below 1200 °C for 30 s to

---

* *Correspondence to: Y. J. Dappe, Service de Physique de l'Etat Condensé (CNRS URA2464), IRAMIS, CEA Saclay, 91191 Gif-Sur-Yvette, Paris, France. E-mail: yannick.dappe@cea.fr*

a   *Synchrotron SOLEIL, Paris, France*

b   *Service de Physique de l'Etat Condensé (CNRS URA2464), IRAMIS, CEA Saclay, Paris, France*

terminate the substrate by the 6√3 × 6√3R30° reconstructed surface. All Si depositions and annealing were made *in situ* and characterized by LEED, ARPES and HRPES.

Both HRPES and ARPES were performed at the soft X-ray TEMPO beamline at Synchrotron SOLEIL.[19] The beamline covers the energy range between 50 and 1500 eV with a resolving power better than 10 000. The spectra were measured using a high energy resolution Scienta SES2002 photoelectron analyzer. The experiments were performed in UHV with a base pressure of 3×10^{-10} mbars. All the presented core level spectra were normalized with respect to the surface contributions. The core level spectra were deconvoluted according to standard curve-fitting procedure.

Ab initio calculations were performed using a very efficient Density Functional Theory (DFT)-localized orbital molecular dynamic technique (FIREBALL).[20–23] Basis sets of sp^3 for C and Si and s for H were used with cutoff radii (in atomic units) $s = 4.5$, $p = 4.5$ (C), $s = 4.8$, $p = 5.4$ (Si) and $s = 4.1$ (H).[24] In this study, we have considered supercells of five layers SiC(0001) with and without Si coverages, with a lateral size roughly corresponding to a 4 × 4 unit cell of graphene. The bottom layer is saturated with hydrogen atoms. On top of each supercell, we have set one 4 × 4 ML of graphene, and we have relaxed the system using a sample of 32 k-points in the Brillouin zone, maintaining the last three layers in bulk positions. A set of 300 special k-points along the path Γ–K–M has been used for the band structure calculations on the relaxed positions

Results and discussion

After a first flash in UHV of the 6H-SiC(0001) (Si-face) substrate below 1200 °C for 30 s, the surface exhibits the typical LEED

pattern of the carbon-terminated 6√3 × 6√3R30° reconstructed surface (Fig. 1a).[25,26] This reconstruction composed of a carbon ML is also called ZLG. This epitaxial graphene layer is rotated by 30° with respect to the SiC-(1 × 1) surface cell. After several Si depositions at room temperature, corresponding to a total Si amount of about 1.75 ML and annealing at 750 °C cycles, this diffraction pattern disappears, exhibiting the bulk SiC-(1 × 1) pattern (Fig. 1c). Epitaxial single-layer graphene diffraction dots should appear close to the position of the 6√3 × 6√3 symmetry.[15] However, working at high energy, the contribution of the graphene mono layer is too weak to be resolved. Notice that the decoupling temperature of the ZLG (750 °C) appears to be lower than the temperature of one ML graphene decoupling (800 °C).[15] Finally, we can also notice an increase of the background intensity that may be attributed to inhomogeneities, unreconstructed surface or randomly distributed Si lying at the surface due to an excess of silicon at the surface.

Core level photoemission spectroscopy measurements are presented in Figs 1b and 1d. The ZLG C1s core level is composed of three components (Fig. 1b): the two components at higher binding energy correspond to the carbon atom of the ZLG partially covalently bonded to the SiC substrate and the component located at lower binding energy corresponds to the SiC bulk.[25] After decoupling, the C1s core level shows two main components (Fig. 1d). The one at higher binding energy exhibits the characteristic asymmetric shape of metallic species and is attributed to the decoupled graphene layer. The component at lower binding energy corresponds to the SiC bulk. This contribution is shifted to the higher kinetic energy in good agreement with literature.[15]

The ARPES measurements presented in Fig. 2 show the valence band structure collected along the Γ–K direction in the graphene

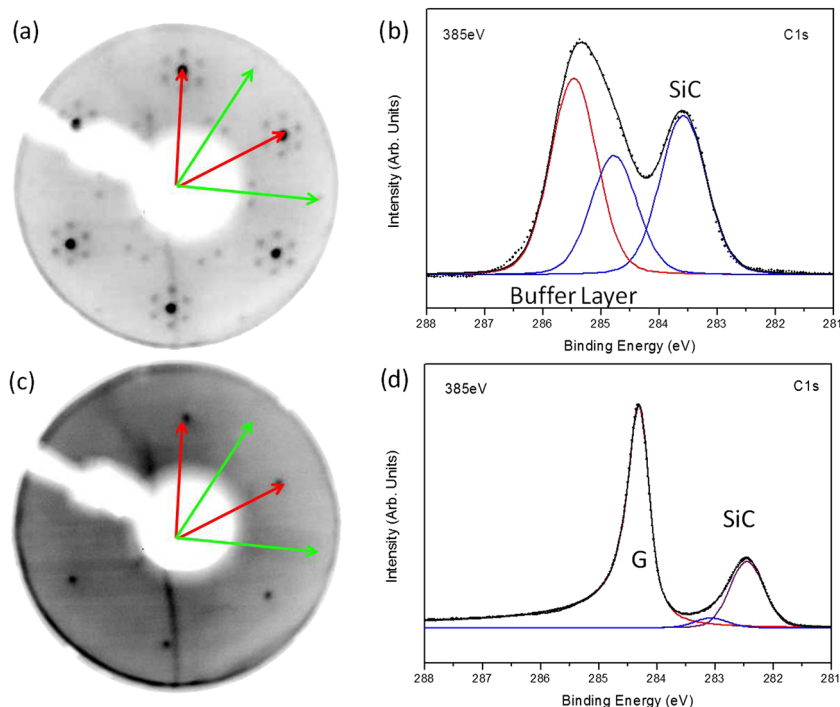**Figure 1.** LEED patterns of the 6H-SiC(0001) surface reconstruction showing buffer layer decoupling. (a) LEED pattern of the 6H-SiC(0001) 6√3 × 6√3R30° buffer layer measured at 170 eV. (c) LEED image taken at 200 eV after several cycles of Si deposition followed by annealing at 750 °C. The image presents a 1 × 1 reconstruction showing the loss of coupling between the buffer layer and the substrate. The short red and long green arrows represent respectively the reciprocal lattice vectors of the Bulk SiC $\left(\vec{B_1}, \vec{B_2} \right)$ and graphene $\left(\vec{G_1}, \vec{G_2} \right)$. Also, the C1s core level spectra measured in surface sensitive mode at photon energy hν = 385 eV, (b) clean (6√3 × 6√3)R30° reconstruction surface and (d) after several cycles of Si deposition followed by annealing at 750 °C.
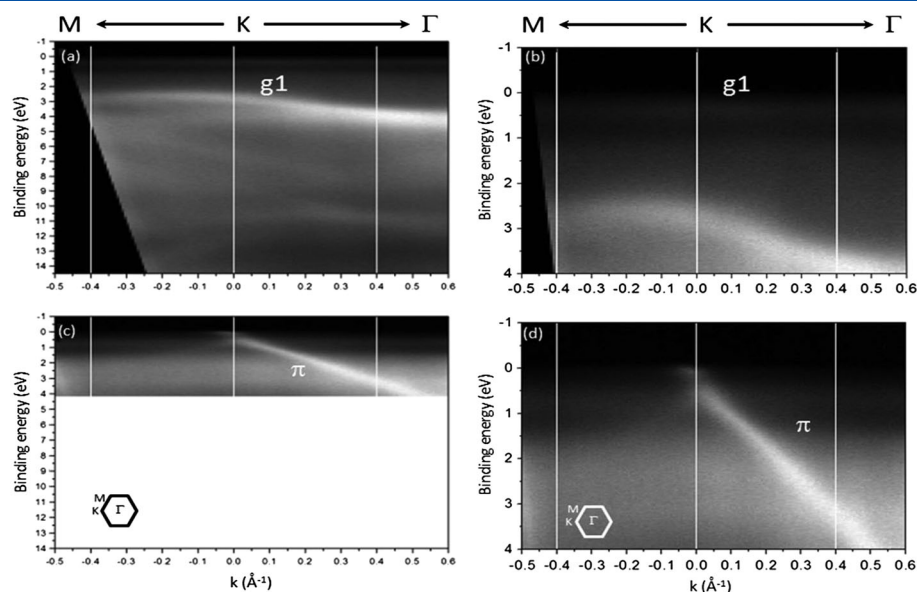
Figure 2. Angle-resolved photoemission spectroscopy spectra presenting the evolution of the electronic properties of the carbon-terminated 6H-SiC (0001) surface during the decoupling process. (a and b) The initial 6H-SiC(0001) $6\sqrt{3} \times 6\sqrt{3}R30°$ buffer layer measured around K-point along the Γ–K–M direction; the white lines point out extrema of the g1 state modulation in k. (c and d) After several cycles of Si deposition and annealing, we obtain a totally decoupled one monolayer graphene.

Brillouin zone for the initial and final steps of Si intercalation process. Figures 2a and 2b present the $6\sqrt{3} \times 6\sqrt{3}R30°$ reconstructed surface bandstructure. As non-metallic surface, no density of states arises at Fermi level, the first localized state g1 being located 0.4 eV below. The non-dispersive g1 state presents an intensity modulation as a function of k. The modulation periodicity appears to be 3/13 of the graphene Γ–K period, corresponding to the second-shortest reciprocal lattice vector of the $6\sqrt{3} \times 6\sqrt{3}R30°$ superstructure.[26] Another small shoulder rising at 1.6 eV below the Fermi level betrays the presence of g2 state partially screened by a continuum at the same energy. Between 2 and 5 eV appears an intense dispersive band presenting 5/13 of graphene periodicity, also observed in cone replica phenomena.[27] Up to 13 eV, the band structure is entangled by several broken structures. We also observe a mini gap opening, characteristic of band folding at reconstruction periodicities wave vector[28] (g1 modulation). The whole structure can be seen as the graphene π-band, modulated by the n-periodic superstructure. This corresponds to the n-folding bandstructure into the 1BZ coming from the incommensurate graphene layer unit cell and $6\sqrt{3} \times 6\sqrt{3}R30°$ unit cells [(13 × 13) graphene unit cell].

After several cycles of silicon deposition and annealing, we have obtained the typical bandstructure of a decoupled graphene layer (Figs 2c and 2d), i.e. the linear dispersion and the Dirac cone. The Dirac point is located at 250 meV below E_F, in good agreement with the values for graphene decoupling by Si intercalation on iridium[29] and graphene on SiC(0001) exposed to air.[30] Consequently, we have calculated an electron density for the decoupled zero graphene layer of about $4.05 \times 10^{12}\,cm^{-2}$ close to the value obtained for epitaxial graphene layer on SiC(0001) exposed to air.[6,30]

To model the ZLG decoupling process and confirm the structural arrangement of the terminated carbon layer during the silicon intercalation, we have calculated the bandstructure for two Si coverages. To calculate the ZLG, we started from truncated 6H-SiC(0001) substrate terminated by the pristine Si with a graphene layer on top. Then, the system has been relaxed – using DFT – until the equilibrium. The final system (Fig. 3a) presents a

covalently bonded graphene-like structure. This configuration is electronically stable because of conservation of mesomeric effects leading to a partial delocalization of the charges. However, the 2D symmetry of the graphene layer is broken, and the metallic character of the film is lost as shown in the band structure calculation (Fig. 3b), explaining the loss in metallicity measured in ARPES.

Moreover, a constrain induced by the covalently sp^3-bonded carbon atoms of the graphene to the silicon atoms of the substrate leads to a distortion of the final carbon layer as shown in theoretical models.[17] Consequently, the calculated C–C distance in the graphene sheet is around 1.55 Å, bearing in mind that periodical calculations also induce an artificial distortion of the graphene network. Our model explains the measured STM images[6,17] reflecting the non-flat behavior of the carbon interface. The Si–C bond distance between the buffer layer and the substrate is equal to 2.14 Å compared with 1.89 Å for the Si–C bond in bulk SiC. Then, extra silicon atoms have been added to the previous interface, and the system has been relaxed again. We have considered here 1.75 ML intercalated Si atoms, following the experimental conditions. Si atoms break the previous Si–C bonds at the interface and link to the substrate Si atom, leading to the release of the carbon atom above, as illustrated in Fig. 3c. Hence, the graphene layer became less highly bonded to the silicon layer below. Calculations including Van der Waals interactions[31,32] show that the graphene layer now lies 2.86 Å above the substrate. This distance is smaller than the interlayer spacing for graphite (3.33–3.35 Å),[33] which explains the measured doping coming from the substrate. We also obtain a C–C distance of 1.55 Å, to be compared with the 8% stretch of the graphene lattice needed to ensure commensurability between graphene and SiC unit cells.[34]

The calculated bands along the Γ–K–M direction exhibit the typical linear dispersion of the Dirac cone of a free-standing graphene layer. For the sake of clarity, we only represent here the contribution to the bandstructure coming from the graphene carbon atoms (Fig. 3d). We also observe disperse bands coming from the small hybridization of graphene states with the SiC
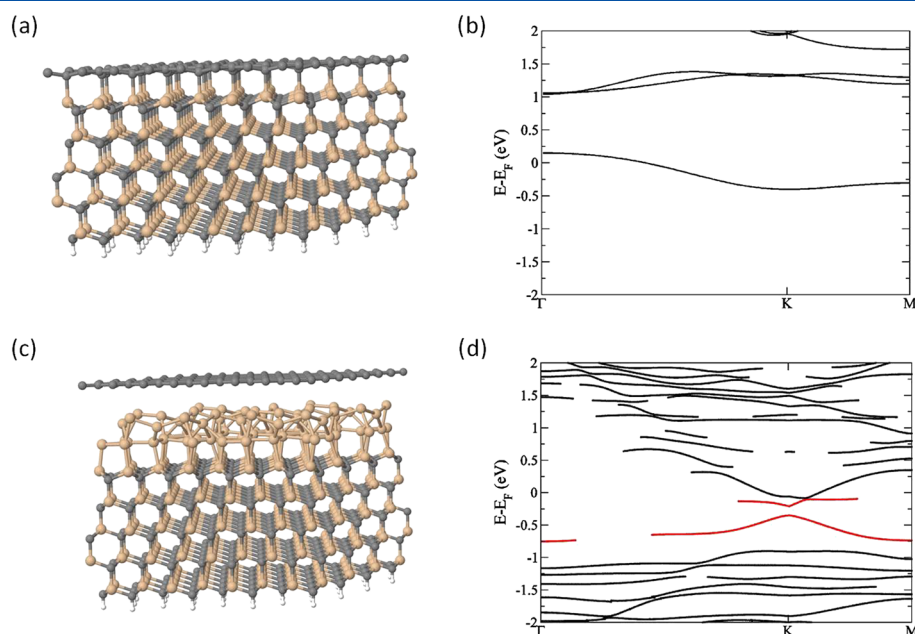
Figure 3. Atomic representation of the initial and final DFT relaxed configurations and calculated band structures along the Γ–K–M direction corresponding to different Si coverages. (a) Representation of graphene layer lying on top of SiC(0001) 1×1 Si-terminated surface. At the equilibrium, covalent Si–C bondings are formed between the graphene layer and the terminated silicon atoms of the substrate. (b) Band structures for the zero-layer graphene on SiC(0001) 1×1. (c) After incorporation of 1.75 ML of Si atoms, the graphene layer stays decoupled from the SiC substrate. (d) Band structures for the decoupled graphene layer in the presence of Si atoms at the interface.

surface states. The small gap that seems to appear in the bandstructure results from the bandfolding induced by the finite size of the unit cell. This gap does not appear experimentally. The Dirac point appears to be around 250 meV below the Fermi level. Consequently, calculations show, in good agreement with experiments, that silicon intercalation leads to decouple zero-layer graphene lying on top of the silicon-terminated SiC substrate. The calculations confirm that the carbon-terminated surface on top of one ML Si initially semiconducting exhibiting no density of states at Fermi level becomes metallic for higher Si coverage, dispersive electronic states crossing the Fermi Level.

Conclusion

By measuring the electronic properties of the ZLG before and after Si intercalation, we have evidenced the transition from semiconductor to metal of the surface. The LEED pattern revealed that a total decoupling of the ZLG can be achieved at 750 °C, a lower temperature compared with the one ML graphene. This result evidences that the presence of an extra graphene layer on top of the ZLG is an impediment to Si intercalation. The resulting decoupled graphene layer exhibits a slight n-doping revealing an electron density of $4.05 \times 10 \, \text{cm}^{-2}$.[12] We have demonstrated that Si intercalation leads to the formation of quasi-free-standing one ML graphene. *Ab initio* calculations corroborate the experimental data.

References

[1] A. H. Castro Neto, F. Guinea, N. M. R. Peres, K. S. Novoselov, A. K. Geim, *Rev. Mod. Phys.* **2009**, *81*, 109.
[2] A. K. Geim, K. S. Novoselov, *Nat. Mater.* **2007**, *6*, 183.
[3] N. Stander, B. Huard, D. Goldhaber-Gordon, *Phys. Rev. Lett.* **2009**, *102*, 026807.
[4] K. I. Bolotin, K. J. Sikes, J. Hone, H. L. Stormer, P. Kim, *Phys. Rev. Lett.* **2008**, *101*, 096802.
[5] C. Berger, X. S. Wu, P. N. First, E. H. Conrad, X. B. Li, M. Sprinkle, J. Hass, F. Varchon, L. Magaud, M. L. Sadowski, M. Potemski, G. Martinez, W. A. de Heer, *Adv. Solid State Phys.* **2008**, *47*, 145.
[6] C. Riedl, C. Coletti, U. Starke, *J. Phys. D Appl. Phys.* **2010**, *43*, 374009.
[7] P. Avouris, C. Dimitrakopoulos, *Mater. Today* **2012**, *15*, 86.
[8] W. A. de Heer, C. Berger, X. S. Wu, P. N. First, E. H. Conrad, X. B. Li, T. B. Li, M. Sprinkle, J. Hass, M. L. Sadowski, M. Potemski, G. Martinez, *Solid State Comm.* **2007**, *143*, 92.
[9] C. Riedl, C. Coletti, T.Iwasaki, A. A. Zakharov, U. Starke, *Phys. Rev. Lett.* **2009**, *103*, 246804.
[10] S. Oida, F. R. McFeely, J. B. Hannon, R. M. Tromp, M. Copel, Z. Chen, Y. Sun, D. B. Farmer, J. Yurkas, *Phys. Rev. B* **2010**, *82*, 041411.
[11] S. L. Wong, H. Huang, Y. Z. Wang, L. Cao, D. C. Qi, I. Santoso, W. Chen, A. T. S. Wee, *ACS Nano* **2011**, *5*, 7662.
[12] I. Gierz, T. Suzuki, R. T. Weitz, D. S. Lee, B. Krauss, C. Riedl, U. Starke, H. Hochst, J. H. Smet, C. R. Ast, K. Kern, *Phys. Rev. B* **2010**, *81*, 235408.
[13] C. Virojanadara, A. A. Zakharov, S. Watcharinyanon, R. Yakimova, L. I. Johansson, *New J. Phys.* **2010**, *12*, 125015.
[14] K. V. Emtsev, A. A. Zakharov, C. Coletti, S. Forti, U. Starke, *Phys. Rev. B* **2011**, *84*, 125423.
[15] C. Xia, S. Watcharinyanon, A. A. Zakharov, R. Yakimova, L. Hultman, L. I. Johansson, C. Virojanadara, *Phys. Rev. B* **2012**, *85*, 045418.
[16] F. Wang, K. Shepperd, J. Hicks, M. S. Nevius, H. Tinkey, A. Tejeda, A. Taleb-Ibrahimi, F. Bertran, P. Le Fevre, D. B. Torrance, P. N. First, W. A. de Heer, A. A. Zakharov, E. H. Conrad, *Phys. Rev. B* **2012**, *85*, 165449.
[17] F. Varchon, P. Mallet, J. Y. Veuillen, L. Magaud, *Phys. Rev. B* **2008**, *77*, 235412.
[18] Y. Qi, S. H. Rhim, G. F. Sun, M. Weinert, L. Li, *Phys. Rev. Lett.* **2010**, *105*, 085502.
[19] F. Polack, M. Silly, C. Chauvet, B. Lagarde, N. Bergeard, M. Izquierdo, O. Chubar, D. Krizmancic, M. Ribbens, J. P. Duval, C. Basset, S. Kubsky, F. Sirotti, *AIP Conf. Proc.* **2010**, *185*, 1234.
[20] J. P. Lewis, K. R. Glaesemann, G. A. Voth, J. Fritsch, A. A. Demkov, J. Ortega, O. F. Sankey, *Phys. Rev. B* **2001**, *64*, 195103.
[21] P. Jelinek, H. Wang, J. P. Lewis, O. F. Sankey, J. Ortega, *Phys. Rev. B* **2005**, *71*, 235101.
[22] O. F. Sankey, D. J. Niklewski, *Phys. Rev. B* **1989**, *40*, 3979.

SURFACE *and* INTERFACE ANALYSIS

[23] J. P. Lewis, P. Jelinek, J. Ortega, A. A. Demkov, D. G. Trabada, B. Haycock, H. Wang, G. Adams, J. K. Tomfohr, E. Abad, D. A. Drabold, *Phys. Status Solidi B* **2011**, *248*, 1989.

[24] M. A. Basanta, Y. J. Dappe, P. Jelinek, J. Ortega, *Comput. Mater. Sci.* **2007**, *39*, 759.

[25] K. V. Emtsev, F. Speck, T. Seyller, L. Ley, J. D. Riley, *Phys. Rev. B* **2008**, *77*, 155303.

[26] S. Y. Zhou, G. H. Gweon, A. V. Fedorov, P. N. First, W. A. De Heer, D. H. Lee, F. Guinea, A. H. C. Neto, A. Lanzara, *Nat. Mater.* **2007**, *6*, 770.

[27] K. Nakatsuji, Y. Shibata, R. Niikura, F. Komori, K. Morita, S. Tanaka, *Phys. Rev. B* **2010**, *82*, 045428.

[28] J. Voit, L. Perfetti, F. Zwick, H. Berger, G. Margaritondo, G. Gruner, H. Hochst, M. Grioni, *Science* **2000**, *290*, 501.

[29] J. H. Mao, L. Huang, Y. Pan, M. Gao, J. F. He, H. T. Zhou, H. M. Guo, Y. Tian, Q. Zou, L. Z. Zhang, H. G. Zhang, Y. L. Wang, S. X. Du, X. J. Zhou, A. H. C. Neto, H. J. Gao, *Appl. Phys. Lett.* **2012**, *100*, 093101.

[30] D. S. Lee, C. Riedl, B. Krauss, K. von Klitzing, U. Starke, J. H. Smet, *Nano Lett.*, **2008,** *8*, 4320.

[31] Y. J. Dappe, M. A. Basanta, F. Flores, J. Ortega, *Phys. Rev. B* **2006**, *74*, 205434.

[32] E. Abad, Y. J. Dappe, J. I. Martinez, F. Flores, J. Ortega, *J. Chem. Phys.* **2011**, *134*, 044701.

[33] O. Hod, *J. Chem. Theor. Comput.* **2012**, *8*, 1360.

[34] F. Varchon, R. Feng, J. Hass, X. Li, B. N. Nguyen, C. Naud, P. Mallet, J. Y. Veuillen, C. Berger, E. H. Conrad, L. Magaud, *Phys. Rev. Lett.* **2007**, *99*, 126805.